Lawrence Berkeley National Laboratory

Title
A SURVEY OF RADIATION DAMAGE IN SEMICONDUCTOR DETECTORS

Permalink
https://escholarship.org/uc/item/0qt1f7r8

Author
Goulding, Fred S.

Publication Date
1971-09-01

LBL-501
Preprint c. 1

A SURVEY OF RADIATION DAMAGE
IN SEMICONDUCTOR DETECTORS

Fred S. Goulding and Richard H. Pehl

September 1971
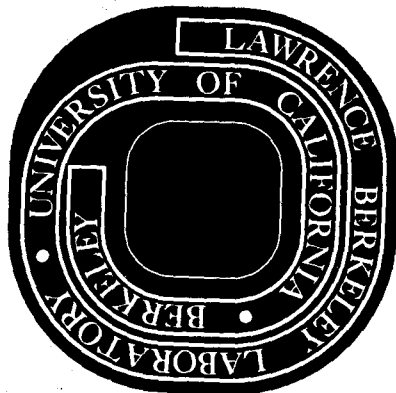
LBL-501

DISCLAIMER

A SURVEY OF RADIATION DAMAGE IN SEMICONDUCTOR DETECTORS[*]

Fred S. Goulding and Richard H. Pehl

Lawrence Berkeley Laboratory
University of California
Berkeley, California 94720

SUMMARY

Examples of radiation damage in lithium-drifted detectors, lithium-drifted silicon detectors, and high-purity germanium detectors are discussed. The general patterns of damage, lithium-precipitation, annealing and recovery of detectors are outlined, and the observations are discussed.

INTRODUCTION

Reviewing relevant papers is an essential part of any survey. In this case, we feel rather like the schoolboy asked to discuss the color of water. He recalled reading of "the blue Mediterranean", "the green lagoons of the south-seas" "the gray Baltic Sea", and "the blood-red ocean reflecting the setting sun". Naturally, he concluded that the color of water depends on both the time and place of observation! The literature on radiation damage in detectors could well lead to an equally valid conclusion.

In an attempt to avoid this result, we will discuss several examples of radiation damage drawn from our own experience in the Lawrence Berkeley Laboratory, emphasising the actual observations, and try to relate them both to data given by other authors, and to possible mechanisms.

LITHIUM-DRIFTED GERMANIUM DETECTORS

For the purpose of this review, data on two detectors representative of many examples seen in our laboratory will be used. Their history is typical, and conclusions drawn from the data can be regarded as generally valid for lithium-drifted germanium detectors.

Detector 40A

This is a planar detector fabricated from the head end of crystal #40, grown by W.L. Hansen at LBL. The slice used was 11 mm thick and about 3 cm in diameter, and was drifted to a depth of 9.5 mm. Its history is outlined in Table 1. The shape of the 1.17 MeV ^{60}Co line at various times[†] is given in Fig. 1, and capacity vs. voltage data are presented in Fig. 2. The following notes relate to various stages in this history.

Stages #1 and 2. These represent the situation before damage. The levelling operation performed between #1 and 2 flattened the capacity-voltage curve, but produced no significant effect on resolution.

Stage #3. Following accidental neutron damage (dose unknown) in pionic X-ray experiments, the ^{60}Co peak exhibited severe tailing characteristic of charge-trapping. The capacity-voltage relationship was not significantly changed from stage #2, so no ionized donors or acceptors (or perhaps equal numbers of each) were produced. Both capacity and spectral data were taken while the detector was still at 77°K.

Stage #4. With the detector still at 77°K, it was scanned from electrode to electrode by collimated γ-rays from a ^{137}Cs source. This scan revealed severe hole trapping. (i.e. performance was best when the γ-ray beam impinged near the p-type side.) This behavior contrasts with that of undamaged detectors made with this material, where very slight electron trapping is observed.

Stage #5. Following a brief warm-up to 25°C, (while still mounted in its holder), the detector was again cooled to 77°K, and tested with ^{60}Co. The trapping now appears to be much worse than in #4, and the capacity-voltage relationship indicates the appearance of either donors or acceptors.

[†] Note that the actual positions of the peaks in this set of curves, and in similar ones in this paper, are not relevant. The peaks have been displaced to clarify the observation of peak shapes.

Stage #6. A repeat of the steps of #5. Surprisingly, trapping was reduced although the concentration of active acceptors or donors has increased. We know from other evidence that acceptors are becoming dominant at this and later stages.

Stage #7. After an additional repeat of the steps of #5 and 6, the trends of stage #6 continued.

Stages #8 through 12. Longer warm-up cycles continued the trends of stages #6 and 7. No data for stages #11 and 12 are given in Fig. 1, as the detector would no longer sustain the 2500 V necessary for direct comparison with earlier stages. Re-etching was not carried out at any stage. After stage #12, the net acceptor concentration in the material corresponded to 10^{11} acceptors/cm^3. This compares with an initial net concentration below 10^9/cm^3, and with total lithium and gallium concentrations of 3 x 10^{14}/cm^3.

Stage #13. Following a reheat to 400°C, and three days drifting under normal drift conditions, the detector was again tested. Its γ-ray performance and capacity-voltage curve were virtually identical to those seen at Stage #2. This represents complete recovery from the effects of damage.

Stages #14 and 15. After additional neutron damage, the detector was recovered again--this time by a four-hour drift followed by levelling overnight at -20°C. Due to improved procedures and better electronics developed during the period of this history, the final detector resolution after stage #14 is slightly better than after stage #2.

The detector is still in use in experiments, and has not suffered significant additional neutron damage.

Detector 3092-B

This planar detector was fabricated from a slice of Hoboken crystal #3092. The drift depth is 9.5 mm. The history of the detector is recounted in Table 2 and in Figs. 3 and 4. As it is similar to that previously described for detector #40A, only three salient features are noted here:

a) After the initial brief warm-up following neutron damage, definite evidence for the prompt production of donors was obtained (stage #4). Scanning tests confirmed this diagnosis. Scans at later stages show a steady increase in acceptor concentration.

b) The degradation in resolution immediately following the first warm-up is less severe than in the case of detector #40A. Furthermore, additional warm-up cycles

(to room temperature) produce almost complete recovery of the detector's energy-resolution, despite the increasing acceptor concentration. We suspect a lower level of neutron damage in this case than in that of detector #40A.

c) While there is slight evidence of uncompensation in the material immediately following damage (still at 77°K), hole trapping (revealed by scanning) is again the main damage symptom.

Discussion

We will now try to relate these experimental results to the work of others. Kraner, et al.[1] irradiated a series of lithium-drifted germanium detectors with 1.0, 5.75, and 16.49 MeV neutrons to levels ranging from about 10^7 to 10^{11} n/cm^2. The irradiations were carried out at 77°K. Measurements of ^{60}Co γ-ray spectra and also capacity vs. voltage behavior were made following the irradiations. Drifting their detectors at +30°C for several days led to similar recovery as observed by us, but no observations equivalent to our brief warm-up cycles were made.

Comparing this work with our own, no significant differences occur in the experimental observations. The fact that severe spectral deterioration occurs for neutron exposure greater than about 10^{10}/cm^2 is established by the work of Kraner et al., and, as in our case, the primary effect at 77°K is the introduction of neutral hole traps. Very low production of acceptors or donors is observed in both sets of detectors when kept at 77°K. We further agree that complete recovery of detectors by lithium-drifting occurs--this implies that precipitation of lithium at damage sites reduces the cross-section of the traps to essentially zero.

Our own work appears to indicate that the prompt effect of heating to room temperature after exposure at 77°K is the production of donors, but precipitation of lithium becomes dominant quickly, and the loss of lithium ions results in p-type material. The improvement in resolution after prolonged periods at 25°C supports the contention that the hole traps produced by radiation are annihilated by lithium precipitation. The lithium precipitation rate, in the case of detector #40A, is about 10^{11} atoms/cm^3/hr. This rate compares with precipitation rates of 4 x 10^8 to 4 x 10^{10} atoms/cm^3/hr quoted by Webb[2] for a wide range of germanium crystals (not damaged by radiation). We believe that high-grade detector material, like our crystal #40, lies at the lower end of Webb's distribution prior to radiation exposure.

The nature of the neutral traps produced by radiation at 77°K is unknown. The primary damage sites may be responsible, but combinations of gallium plus vacancies or lithium plus vacancies may be involved. These latter mechanisms demand migration of vacancies at 77°K. It is of interest to examine high-purity germanium detectors where the acceptor and/or donor levels are 10^4 times less than in lithium-drifted material, and where the possibility of acceptor/donor-defect interactions is negligible.

HIGH-PURITY GERMANIUM DETECTORS

Work on high-purity germanium detectors has been very limited, and data on radiation damage is almost non-existent. However, we will discuss one case of a detector damaged in an experiment at LBL, and will make some comparisons with the results given by Llacer and Kraner[3], who have conducted radiation-damage experiments on five small detectors. As there is some possibility that lithium ions are involved in the degradation mechanism in lithium-drifted detectors, one might suspect that the degradation in high-purity germanium detectors could be smaller than those in lithium-drifted detectors. This belief was the reason for some of our early interest in pure germanium, but we will see that our optimism was probably misplaced.

Detector 127-13

This detector is 1 x 1 cm in area, 6 mm thick, and is made from p-type material having an acceptor concentration of 5 x 10^{10}/cm^3 (germanium produced by W. L. Hansen). It was intended for use in a study of the energy-resolution attainable with high-purity germanium detectors stopping 40 MeV protons, and was used in an experiment in December 1970. An outline of the history of the detector is given in Table 3, capacity-voltage data is given in Fig. 5, and spectral data obtained at various stages is given in Fig. 7. This data includes the shape of the ^{60}Co 1.17 MeV line at some stages, and also that of the ^{207}Bi 1.063 MeV γ-ray and L and M conversion-electron lines at other stages. the ^{207}Bi measurements provide data on the detector dead-layer parameters. The following brief observations amplify the comments in Table 3.

Stage #1. Prior to use in the cyclotron experiment, the ^{207}Bi spectrum was measured with 1250 V on the detector. Excellent resolution was obtained. The capacity-voltage curve, and the value of punch-through voltage, determined by observation of electrons, agree with the impurity concentration (5 x 10^{10}) determined by resistivity measurements on the original crystal. The capacity-voltage relationship conformed to a $C \propto V^{-1/2}$ law.

During the 40 MeV proton experiment, the detector was accidentally exposed to the direct beam; the total exposure is believed to have been between 10^{11} and 10^{12} particles in a collimated rectangular region about 6 x 4 mm in area. The radiation damage prevented further observations from being made with this detector during the experiment; it was replaced by another high-purity detector that yielded a FWHM resolution of < 20 keV on the 40 MeV protons.

Stage #2. The first observations on the detector following damage were made after two weeks, during which time the detector was at room temperature. At this point, ^{60}Co peaks showed severe broadening and tailing. Furthermore, the capacity-voltage relationship no longer obeyed a $C \propto V^{-1/2}$ law, and the apparent value of detector capacity at high voltages had increased by at least 2 pF compared with its pre-irradiation value. We believe that radiation damage caused the central region of the detector to be heavily p-type at this stage, as shown in Fig. 6A.

Stage #3. A 6-minute annealing cycle was performed at 400°C, and the capacity-voltage relationship was much improved when compared with stage #2. However, the electron/gamma ratio was much smaller than observed in the pre-irradiation test. This can be seen by comparing stages #3 and 1 in Fig. 7. This is explained by comparing the shapes of the collimators used in the proton experiment, and in the ^{207}Bi electron measurements (see Fig. 6B). The reduced electron efficiency may be due to a dead layer within the region defined by the electron collimator--this is consistent with the damaged region shown in Fig. 6A being p-type at stage #3.

Stages #4, 5, and 6. Successive prolonged periods (6, 12, and 24 min) of annealing at 400°C finally restored the original electron/gamma ratio.

Stage #7. The final ^{60}Co spectrum shows complete recovery of the detector despite the gross damage introduced during the cyclotron experiment.

Discussion

We will now try to relate these results to the work of Llacer and Kraner, and to the results presented earlier on lithium-drifted germanium detectors. The ^{60}Co peak spectral data and capacity-voltage curves for their detector 373-1 are reproduced in Figs. 8, 9, and 10. Their detector was fabricated from p-type material having an initial concentration of 4 to 5 x 10^{10} acceptors/cm^3. Its area was about 1 cm^2 and thickness only 3 mm (the small thickness makes observation of trapping effects more difficult than for thicker detectors). The detector was irradiated with 1.6 MeV neutrons, and γ-ray measurements were made at various stages during the irradiation with the results shown in Fig. 8.

Following the final irradiation (8×10^{10} n/cm^2), the detector was allowed to stand at 77°K for 24 hours; its γ-ray response was then as shown in the curve marked "FINAL" in Fig. 8. Some annealing is evident even at 77°K.

The detector was then allowed to anneal at room temperature for 24 hours, then measured at 77°K; successive annealing cycles were then carried out, each followed by testing at 77°K. The spectral data of Fig. 9, and capacity-voltage data of Fig. 10, show the results of these annealing cycles.

Combining these observations with our own, the following conclusions are the only clear ones that can be drawn:

a) Severe radiation damage effects appear for neutron (or high-energy proton) doses greater than about 10^{10} neutrons/cm^2.

b) After a short period at room temperature, a substantial increase in acceptor concentration is observed. Detector 373-1 exhibited a level of 5×10^{11} acceptors/cm^3. The measurements available do not indicate whether the additional acceptors are present at 77°K immediately after irradiation.

c) Annealing at high temperature completely heals the damage--at least as far as its effect on trapping, and on the acceptor concentration is concerned. In our case, about one hour at 400°C was used, while 1 to 2 hours at 200 and 250°C was adequate in Llacer and Kraner's detector. Their results suggest that the final detector is significantly better after damage and repair, than prior to damage. They observe a similar improvement in all five detectors tested. This observation may be related to Hansen's suggestion that the acceptors seen in high-purity germanium may be due to vacancies.[4]

The relationship of these results to those observed with lithium-drifted germanium detectors is obscured by the lack of several important observations. For example, no capacity-voltage measurement has been made on high-purity germanium detectors following irradiation while the detector is still at 77°K. Also, the partial recovery at 77°K observed in Llacer and Kraner's detector implies that the spectral degradation resulting from irradiation might well exhibit a dependence on neutron dose-rate as well as total flux. This makes difficult any comparison of devices damaged in brief exposures (all the high-purity germanium results are in this category) with those where damage has occured over a long period (such as the lithium-drifted detectors we have studied). Two tentative suggestions can be made, based on comparing the high-purity germanium results with those for lithium-drifted detectors:

a) The threshold dose for severe damage effects is similar in the two cases. This strongly suggests that production of neutral hole-traps will be the initial mechanism observed in spectroscopy experiments with either type of detector. If this is true, it indicates that vacancy plus lithium or vacancy plus gallium pairs are not a factor in the degradation process in lithium-drifted detectors when maintained at 77°K.

b) Raising the detector temperature to 25°C for a significant length of time result in generation of acceptors in both cases. While lithium-precipitation must be a major factor in this process in lithium-drifted detectors, the pure-germanium work suggests that a damage process basic to the germanium also contributes acceptors.

The mechanisms used to repair damage in the two cases are quite different. In lithium-drifted detectors, we assume that lithium ions precipitate at damage sites annihilating the traps, and that each site can probably accept only one lithium atom. The redrift-repair process presumably replaces the lithium lost by precipitation. On the other hand, the high-temperature anneal process used to repair pure-germanium detectors (which is not applicable to lithium-drifted detectors) must involve reassociation of vacancy-interstitial pairs produced by the radiation damage. It is surprising that the reassociation is so complete; perhaps it would not be if the damage were uniformly distributed. In both cases studied here, the damage produced by individual collisions of neutrons or protons is locally intense, and the high-density damage clusters may be easier to anneal than the distributed isolated damage sites characteristic of γ-ray damage.

LITHIUM-DRIFTED SILICON DETECTORS

At the present time, no information is available on the damage effects in lithium-drifted silicon detectors damaged and used at 77°K. However, a wealth of experimental data is available on such detectors used at, or near, room temperature in accelerator experiments, where copious quantities of fast neutrons are produced. Basic data on semiconductor aspects of the damage is lacking, but adequate practical pictures have emerged. These effects were summarized by Goulding and Lothrop.[5] The conclusions, modified by more recent data, are as follows:

a) The primary observable effect of damage is a loss of compensation in the drifted region. This is due to lithium-precipitation at damage sites--although the recent

results on pure-germanium detectors make one cautious about ascribing all the acceptors to lithium-precipitation.

Lithium-precipitation is a relatively slow process, so degradation continues after the end of an experiment; a detector may perform well during a 1- or 2-day experiment, but then be useless when required a week or two later.

b) The slow departure from exact compensation in the drifted region produced by lithium-precipitation at damage sites during an experiment causes a change in the electric field distribution. Consequently, a slow change occurs in the collection-time of carriers as damage accumulates; this can be important if the device is being used in coincidence or timing experiments. Timing changes are usually the earliest indicator of damage.

c) When sufficient lithium has precipitated at the damage sites, the applied detector voltage becomes inadequate to deplete the whole detector. A dead-layer is thereby produced at the particle-entrance face, and the energy resolution for particles passing through this face suffers accordingly.

d) The threshold level for damage clearly depends on the sensitivity of observation, but, as with lithium-drifted germanium detectors, the range of 10^{10} n/cm^2 represents a good estimate.

Repair of damage in lithium-drifted silicon detectors can be accomplished by redrifting lithium in a similar way to that used for germanium detectors. However, the simpler fabrication of lithium-drifted silicon detectors makes their repair less important than that of germanium detectors. In our laboratory, repair of damage by redrifting is only used for thick silicon detectors (> 3 mm).

Recent studies by Kool et al.[6] of lithium-precipitation in detectors damaged by γ-ray irradiation has yielded some basic data on the precipitation mechanism. The experiments were carried-out with lithium-drifted silicon slices exposed to a total [60]Co γ-ray dose of 3 x 10^{16} γ/cm^2, introducing a defect density near 10^{13}/cm^3. The resistivity was then measured for a long time after irradiation using a Hall Effect apparatus. Three types of silicon were tested, two being similar to the materials used for radiation detectors, while the third contained a high oxygen concentration.

For a single type of defect, present at a concentration well below that of lithium in the silicon, one might expect that the number of defects filled by precipated lithium ions would obey an exponential law with time. As expressed by Kool et al.[6], the acceptor concentration would obey the law:

$$p(\infty) - p(t) = \left\{ p(\infty) - p(o) \right\} \exp\left(-t/\tau\right) \quad (1)$$

where $p(\infty)$, $p(t)$, $p(o)$ represent the acceptor concentrations at infinite time, time t, and zero time respectively.

The time constant τ should be related to the temperature, since the lithium diffusion coefficient increases with temperature. This increases the probability of a lithium ion finding a precipitation site, and speeds up the precipitation rate. Figure 11, extracted from the paper by Kool et al., shows the behavior of the acceptor concentration with time for slices held at 30°C and 50°C. These results are in agreement with Eq. (1), indicating that a single type of precipitation site is present. The time constants of the precipitation process are roughly 250 hours at 30°C, and 40 hours at 50°C. We note that these times are similar to those encountered in detectors damaged by neutrons in accelerator experiments.

Using their data, Kool et al.[6] show that the cross-section of the precipitation site is very small (radius ~2.5 x 10^{-8} cm); therefore Coulomb forces are not involved in the process.

CONCLUSION

As shown in our discussion of each type of detector, we lack much of the data required to obtain a detailed picture of the radiation damage process, and of its subsequent healing. However, the radiation levels at which damage becomes important are known, the effects on experiments can be anticipated, and repair techniques have been developed. It is unfortunate that so little effort has been expended in understanding the processes involved in an important experimental tool.

ACKNOWLEDGMENTS

REFERENCES

1. H. W. Kraner, C. Chasman, and K. W. Jones, Nucl. Instr. and Methods 62, 173 (1968).

2. P. P. Webb, IEEE Trans. Nucl. Sci. NS-15, No. 3, 321 (1968).

3. J. Llacer and H. W. Kraner, Neutron Damage and Annealing in High-Purity Germanium Detectors, Brookhaven National Laboratory Report BNL-16142 (1971).

4. W. L. Hansen, Observation of Isolated Defects in High-Purity Germanium, Lawrence Radiation Laboratory Report UCRL-20807 (1971).

5. F. S. Goulding and R. P. Lothrop, Some Observations of Radiation Damage in Lithium-Drifted Silicon Detectors, Semiconductor Nuclear-Particle Detectors and Circuits, National Academy of Sciences Publication #1593, p. 337 (1969).

6. W. H. Kool, J. J. Goedbloed, and C. A. J. Ammerlaan, J. App. Phys. 42, 2024 (1971).

TABLE 1 : DETECTOR # 40A HISTORY

DATA SET #	DATE	NOTES
1	4-24-68	FIRST TEST (DRIFT 9.5mm)
		STORED THEN LEVELLED
2	5-1-68	TEST PRIOR TO USE
		NEUTRON DAMAGE IN MESIC
		X-RAY EXPERIMENTS
3	5-28-68	TESTED WHILE AT 77°K
4	5-28-68	SCAN TESTS AT 77°K
5	5-28-68	AFTER BRIEF WARM-UP TO 25°C
6	5-29-68	AFTER FURTHER BRIEF
		WARM-UP
7	5-29-68	AFTER FURTHER BRIEF WARM-UP
8	5-29-68	AFTER FURTHER 5 MIN. WARM-UP
9	5-31-68	AFTER FURTHER 5 MIN WARM-UP
10	5-31-68	AFTER FURTHER 8 MIN WARM-UP
11	5-31-68	AFTER FURTHER 12 MIN WARM-UP
12	5-31-68	AFTER FURTHER 15 MIN WARM-UP
		REHEAT TO 400°C
		AND REDRIFT 3 DAYS
13	6-7-68	RETEST-THEN
		TO HILAC FOR EXPT'S.
14	5-25-69	TESTED AFTER NEUTRON DAMAGE
15	5-26-69	AFTER 4 HOURS DRIFT
		AND LEVELLING
		IN USE AT HILAC UNTIL NOW

N.B: ALL TESTS CARRIED OUT
WITH DETECTOR AT 77°K

XBL 7110-1519

TABLE 2: DETECTOR #3092-B HISTORY

DATA SET #	DATE	NOTES
1	7-10-67	INITIAL TEST (DRIFT 8mm)
2	5-8-68	TEST AFTER NEUTRON DAMAGE
3	5-8-68	SCAN TESTS
4	5-9-68	AFTER BRIEF WARM-UP TO 25°C
5	5-9-68	AFTER FURTHER BRIEF
		WARM-UP
6	5-9-68	AFTER FURTHER 30 MIN
		WARM-UP
7	5-9-68	SCAN TESTS
8	5-9-68	AFTER FURTHER 30 MIN
		WARM-UP
9	5-10-68	AFTER FURTHER 30 MIN
		WARM-UP
10	5-10-68	AFTER FURTHER 30 MIN
		WARM-UP
11	6-4-68	AFTER REHEAT (400°C)
		REDRIFT AND LEVEL
12	9-17-68	AFTER NEUTRON DAMAGE
13	9-17-68	SCAN TESTS
14	9-17-68	AFTER 30 MIN WARM-UP
DRIFTED REGION IS NOW NEAR TO THE BACK TESTING IS THEREFORE ENDED AT THIS POINT		

N.B: ALL TESTS CARRIED OUT WITH DETECTOR
    AT 77°K

XBL 7110-1517

TABLE 3: HIGH-PURITY Ge DETECTOR
#127-13 HISTORY

DATA SET #	DATE	NOTES
1	12-18-70	INITIAL TEST (Bi 207)
	12-22-70	USED IN CYCLOTRON 42 MeV
		PROTON RUN. EXPOSED TO
		ABOUT 10^{11} p/cm^2 IN REGION
		6mm × 4mm IN AREA
2	1-4-71	Co 60 TEST AFTER 2 WEEKS
		AT ROOM TEMP.
3	1-7-71	AFTER 6 MIN AT 400°C
		(Bi 207)
4	1-8-71	AFTER FURTHER 6 MIN
		AT 400°C
5	1-11-71	AFTER FURTHER 12 MIN
		AT 400°C
6	1-11-71	AFTER FURTHER 24 MIN
		AT 400°C
7	2-17-71	Co 60 SPECTRUM
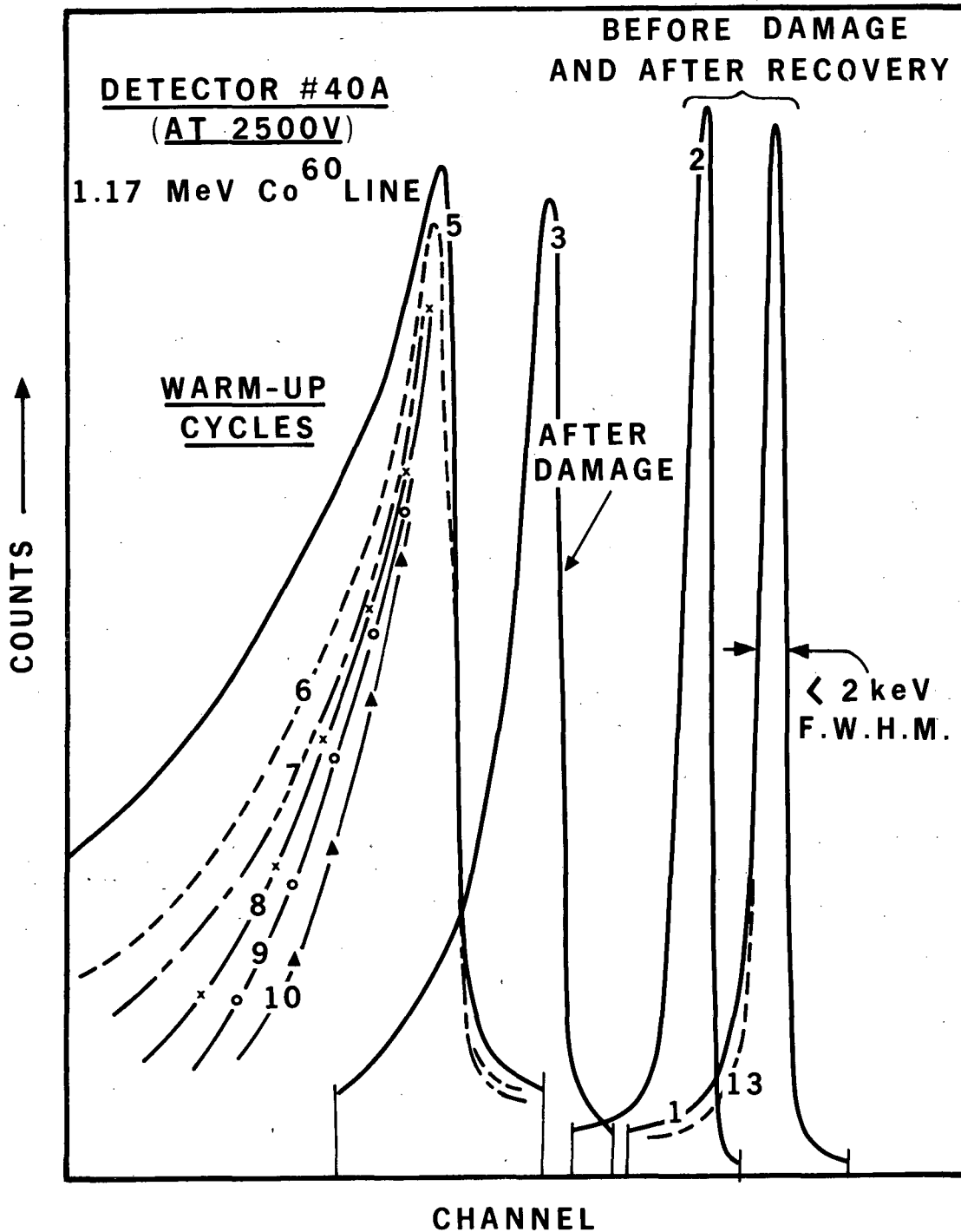
XBL 7110-1518

Fig. 1. Detector #40A; showing the shape of 1.17 MeV ^{60}Co peak at various stages (see Table 1). No relevance should be attached to the peak position.
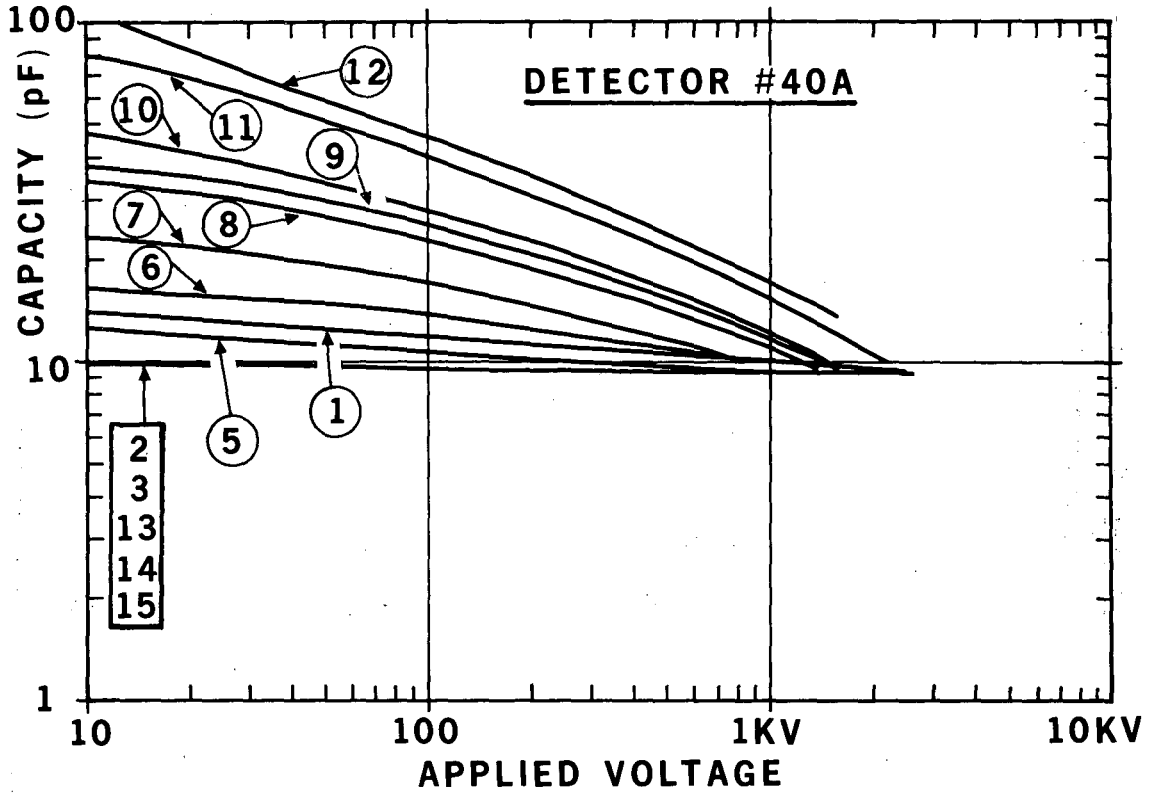
Fig. 2. Detector #40A; capacity-voltage
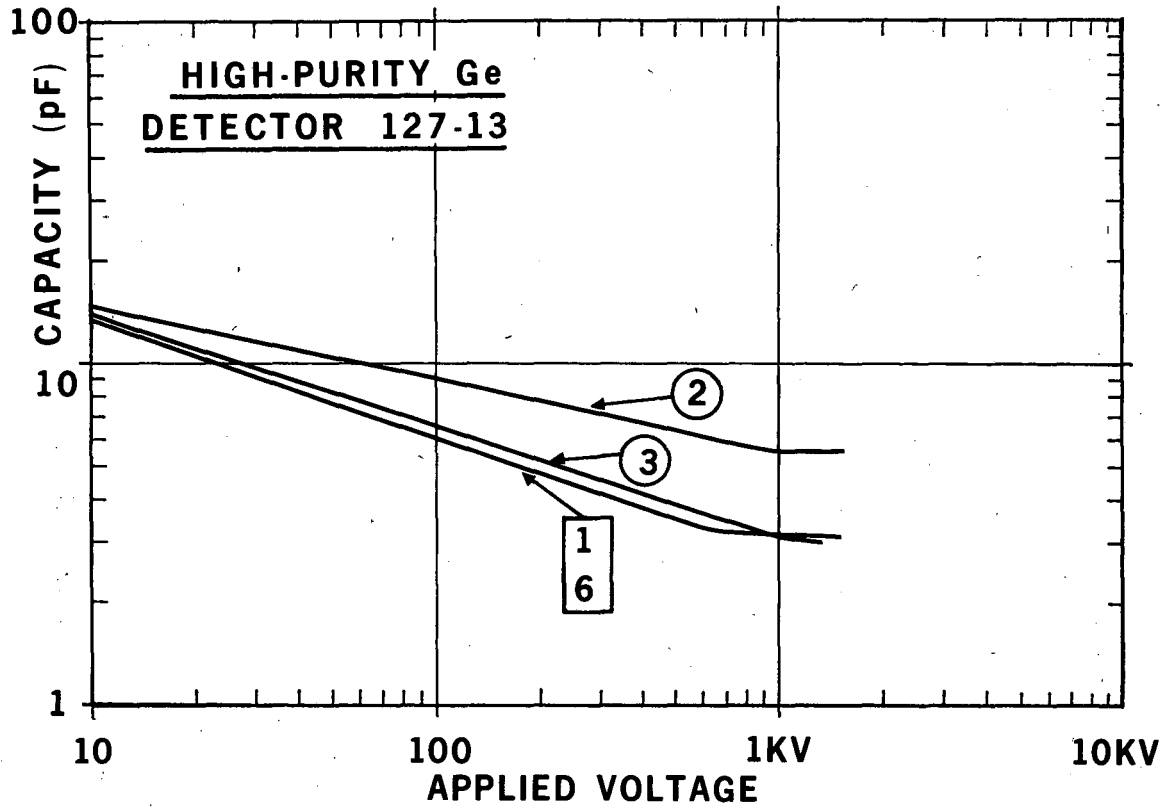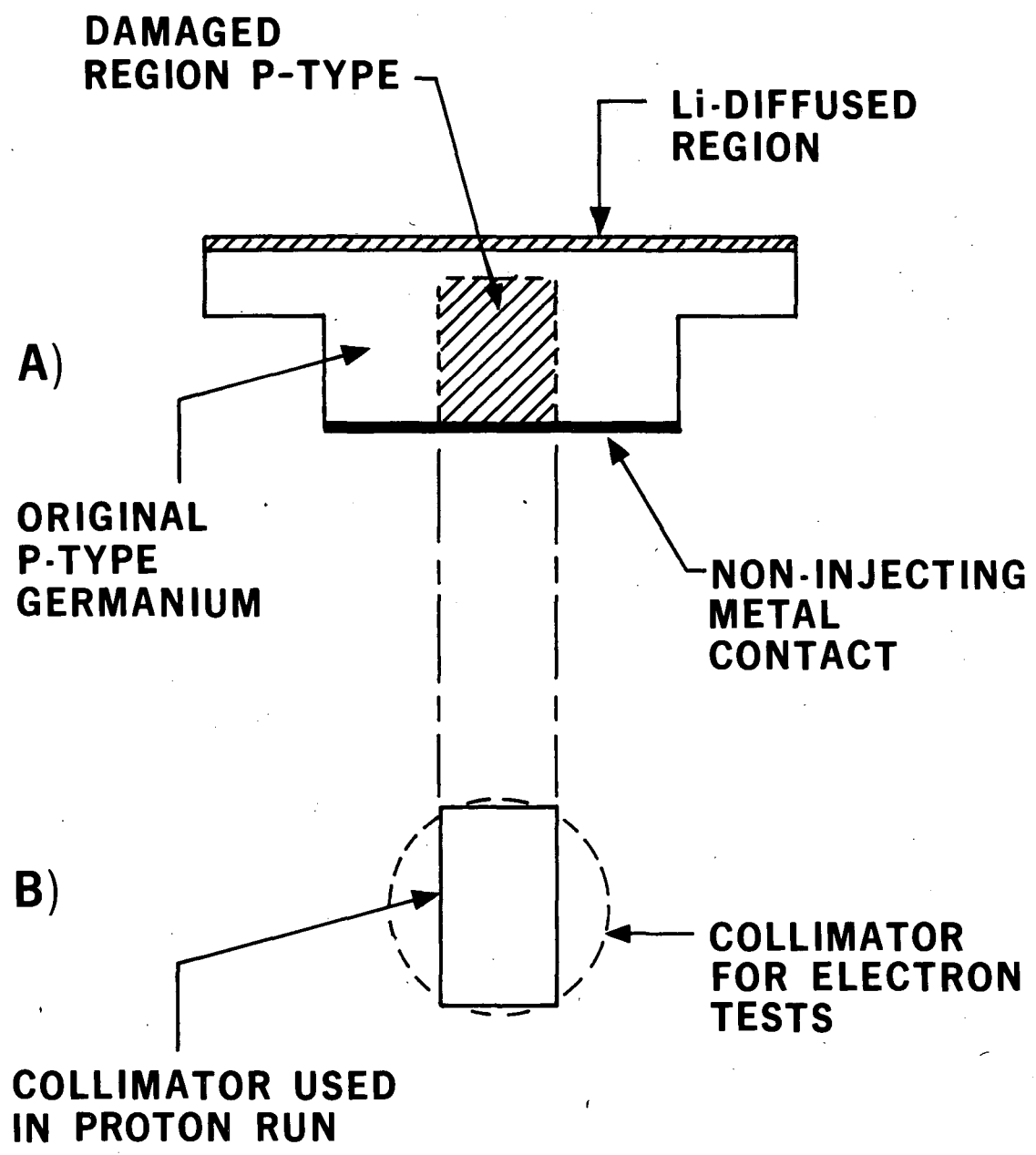relationship at various stages
(see Table 1).

DETECTOR 3092B (AT 2000V)

1.17 MeV Co^{60} LINE

WARM-UP CYCLES

4

5

8

6

1

11

2
AFTER DAMAGE

1
INITIAL & AFTER RECOVERY

4.06 keV

<2keV FWHM

COUNTS ⟶

CHANNEL
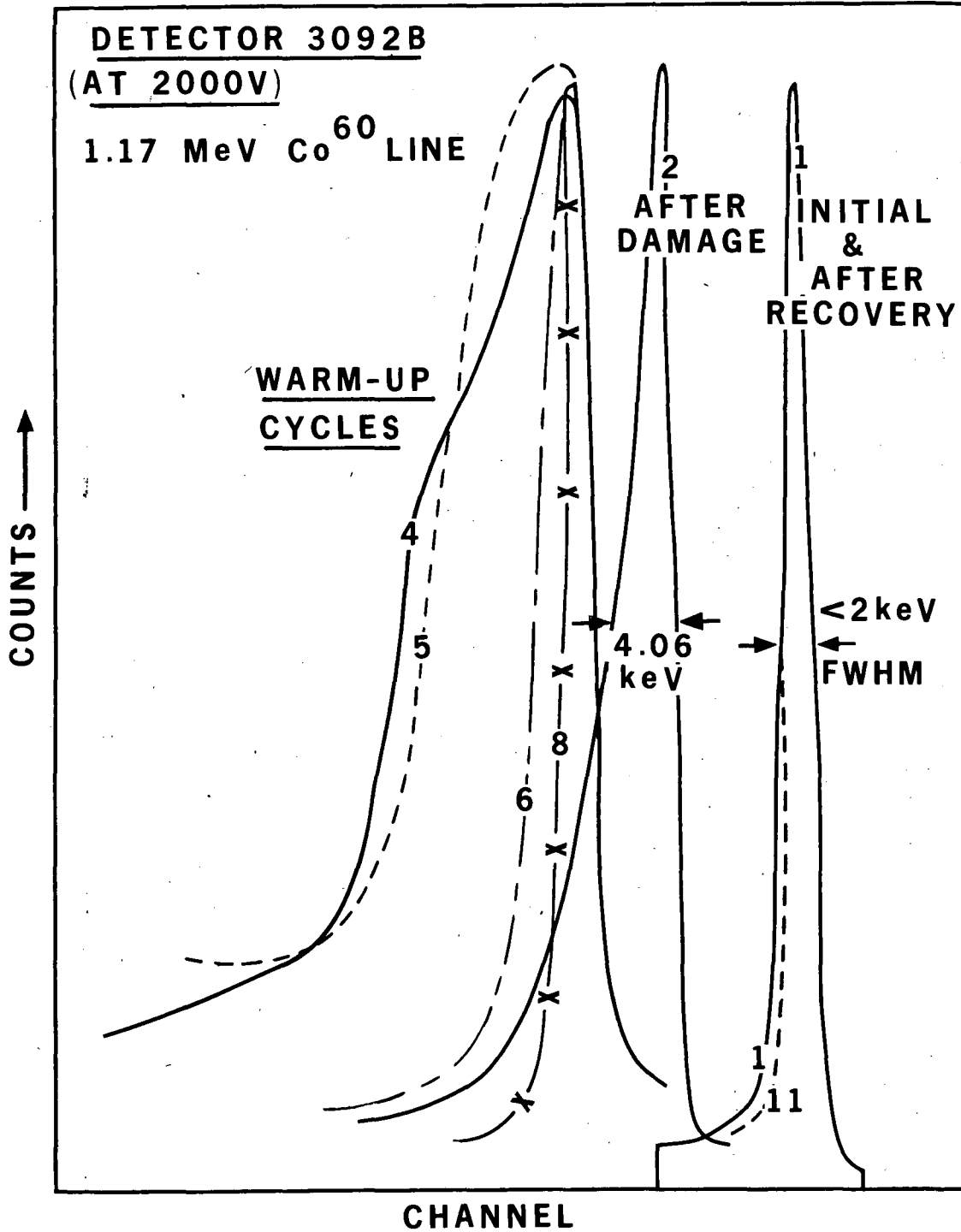
XBL 7110-1524

Fig. 3. Detector #3092B; showing the shape of 1.17 MeV ^{60}Co peak at various stages (see Table 2). No relevance should be attached to the peak position.
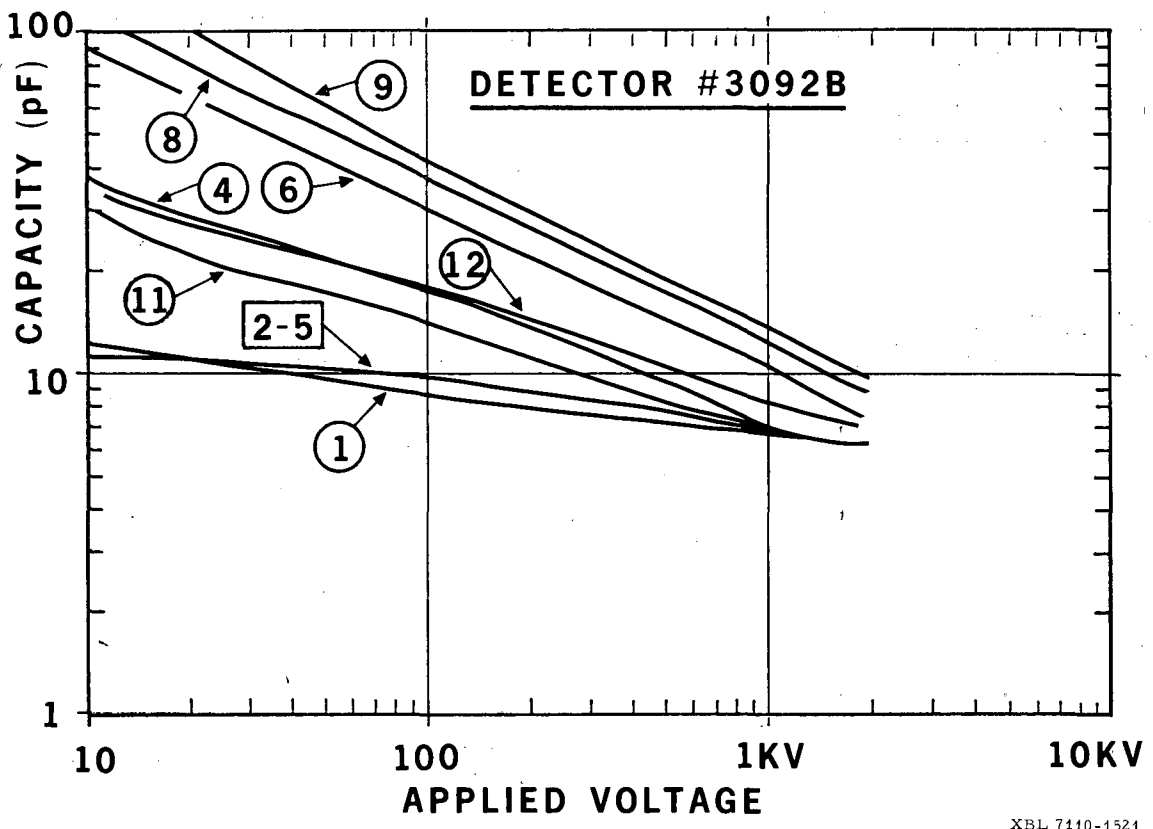
Fig. 4. Detector #3092B; capacity-voltage
         relationship at various stages
         (see Table 2).

Fig. 5. Detector #127-13; capacity-voltage
relationship at various stages
(see Table 3).

**DAMAGED
REGION P-TYPE**   **Li·DIFFUSED
REGION**

A)

**ORIGINAL
P·TYPE
GERMANIUM**

**NON·INJECTING
METAL
CONTACT**

B)

**COLLIMATOR
FOR ELECTRON
TESTS**

**COLLIMATOR USED
IN PROTON RUN**

XBL 7110-1527

Fig. 6. A.   Probable model for damage in
             detector #127-13.

      B.   Arrangement of collimators for
           proton experiment and ^{207}Bi
           electron test on detector
           #127-13.
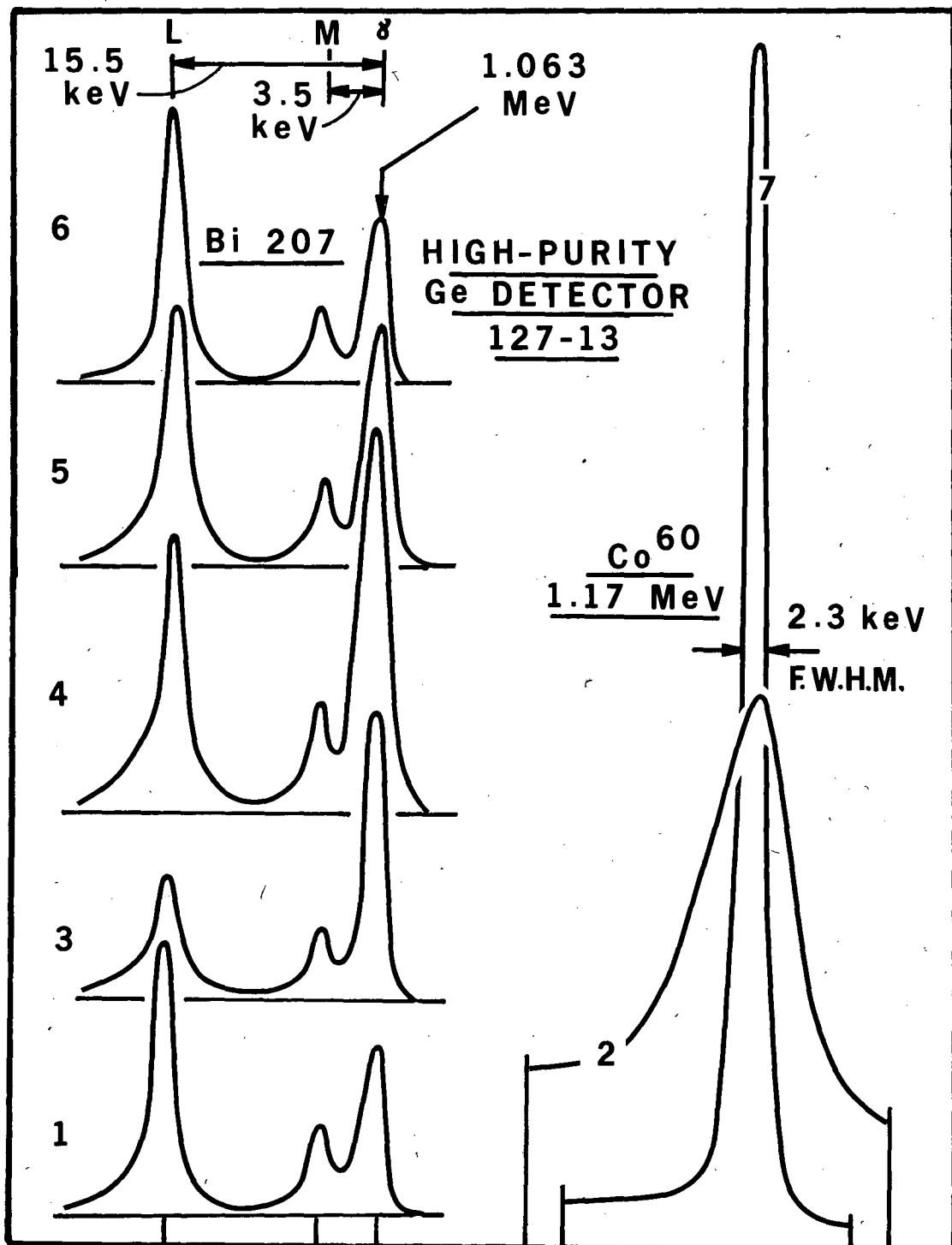
Fig. 7. Detector #127-13; ^{60}Co and ^{207}Bi
         peaks at various stages (see
         Table 3). The relative heights
         of γ- and K-conversion electron
         lines indicate the effect of a
         dead layer in the entry window.

XBL 7110-1525
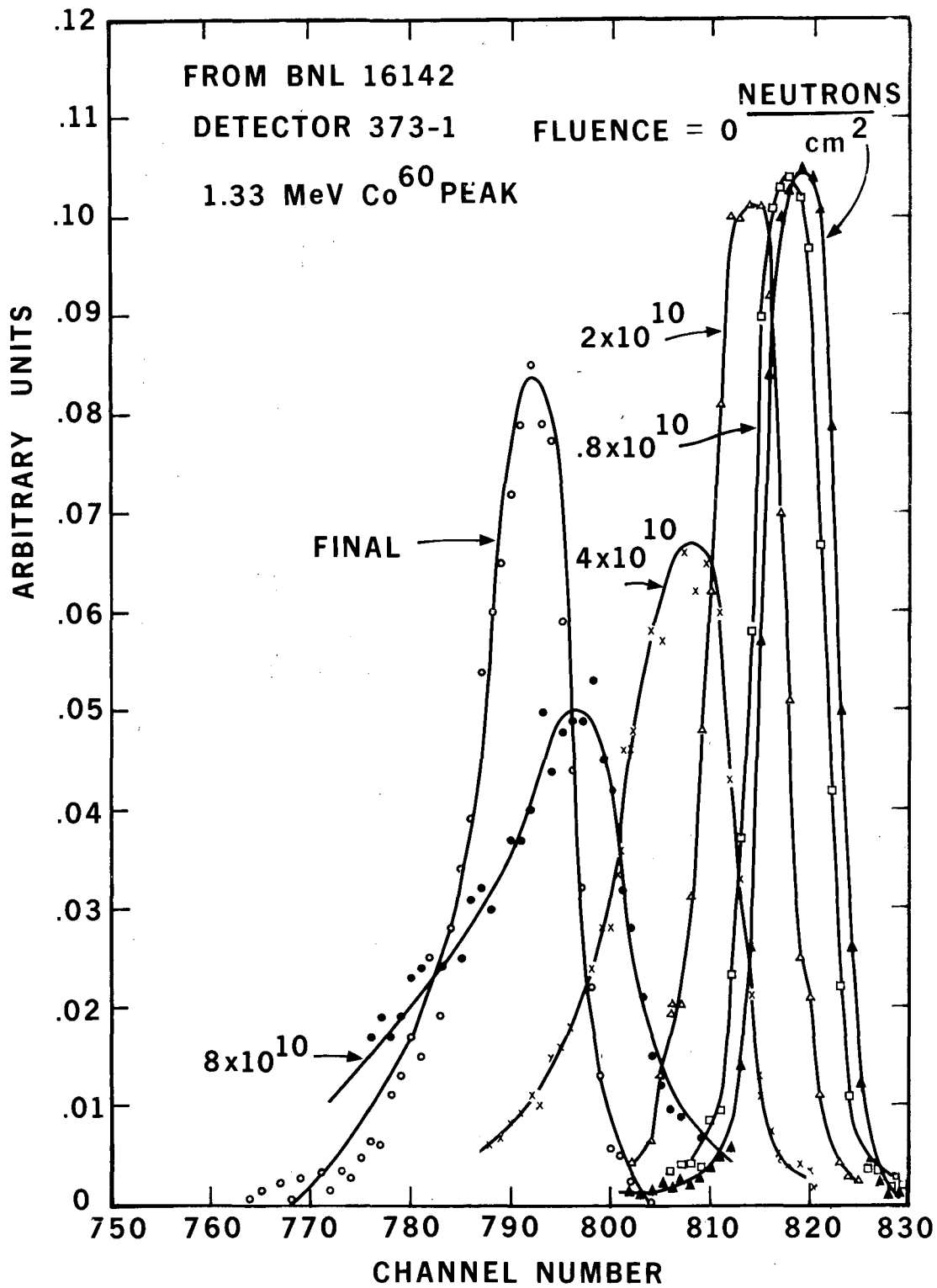
Fig. 8.   Detector #373-1; showing the ^{60}Co
          peak during irradiation (see Ref. 3).
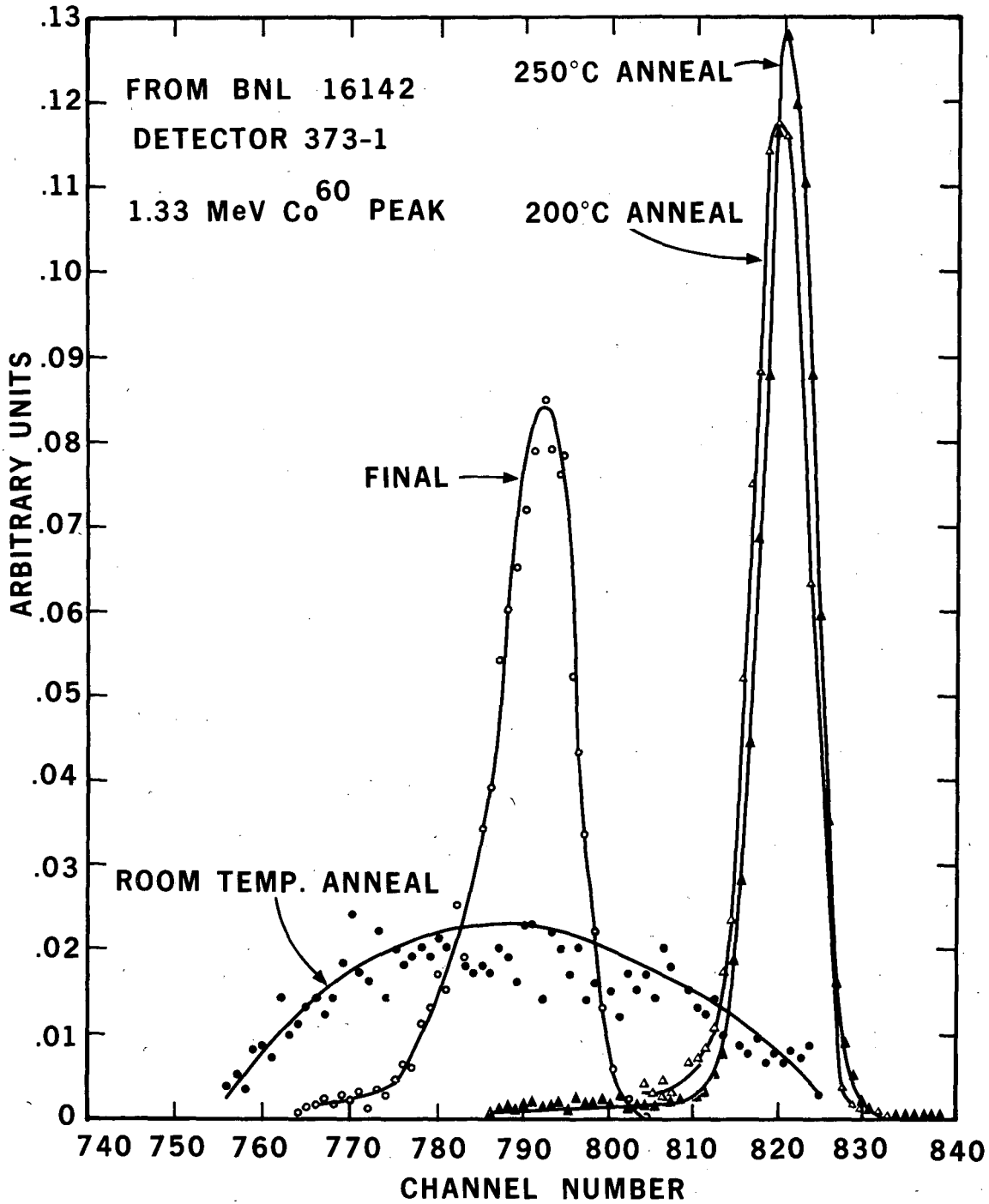
Fig. 9. Detector #373-1; showing the ^{60}Co
         peak during annealing (see Ref. 3).
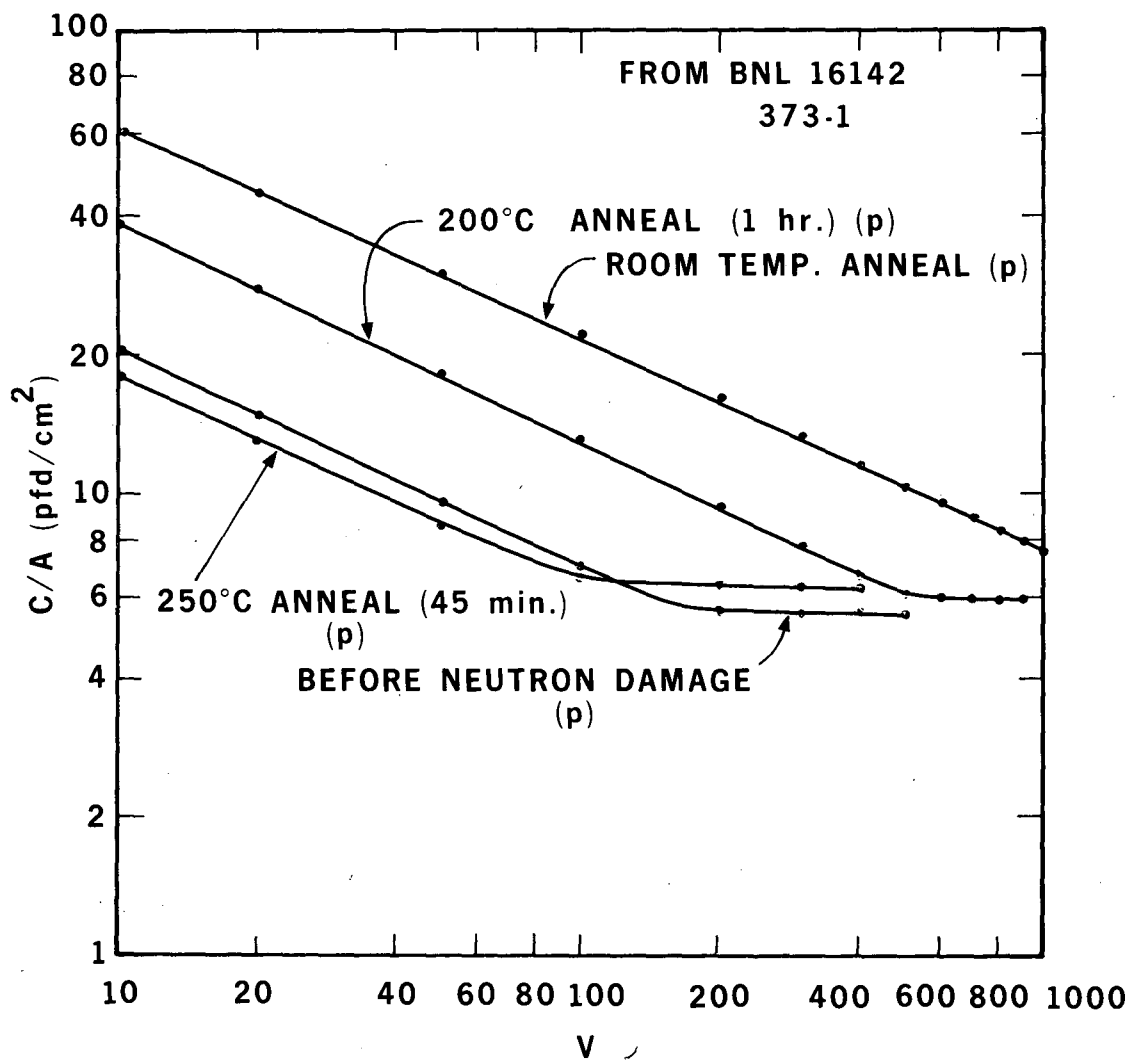
XBL 7110-1543

Fig. 10.   Detector #373-1; capacity-voltage
          relationship during annealing.
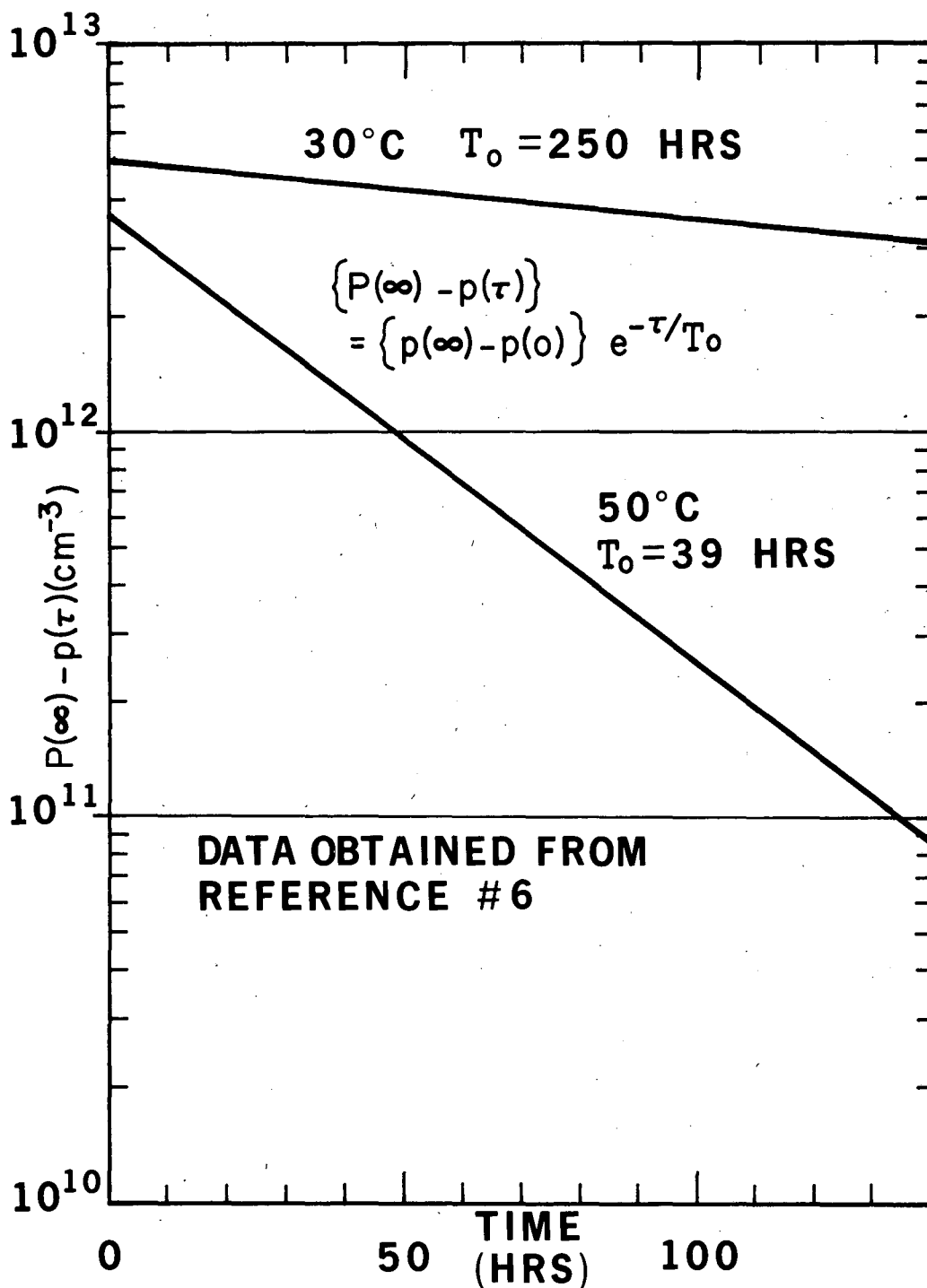
Fig. 11. Lithium precipitation in radiation damaged silicon (see Ref. 6). The vertical scale represents the number of damage sites not filled by lithium atoms. The time behavior is shown for samples at 30°C and 50°C.